Chemical Engineering Science 137 (2015) 243–253

Contents lists available at ScienceDirect

Chemical Engineering Science

journal homepage: www.elsevier.com/locate/ces

Airlift bioreactor for biological applications with microbubble mediated transport processes

Mahmood K.H. AL-Mashhadani [a,*], Stephen J. Wilkinson [b], William B. Zimmerman [c]

[a] Department of Chemical Engineering, College of Engineering, University of Baghdad, Baghdad, Iraq
[b] Department of Chemical Engineering, University of Chester, Thornton Science Park, Pool Lane, Ince, Chester CH2 4NU, UK
[c] Department of Chemical and Biological Engineering, University of Sheffield, Mappin Street, Sheffield S1 3JD, UK

HIGHLIGHTS

- Microbubbles increase the mixing efficiency in airlift bioreactors.
- Dispersal of gas phase throughout the ALR occurs with decreasing the bubble size.
- Phase slip velocity decreases with smaller bubble size as gas rise rate decreases.

GRAPHICAL ABSTRACT

Snapshots of gas concentration at different bubble diameter after steady state

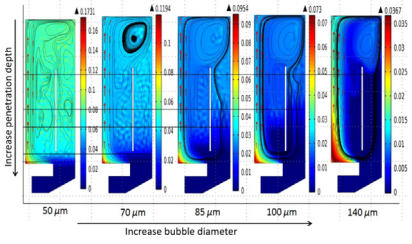

Snapshots of gas concentration at different bubble diameter after steady state

ARTICLE INFO

Article history:
Received 8 December 2014
Received in revised form
23 April 2015
Accepted 10 June 2015
Available online 25 June 2015

Keywords:
Microbubbles
Fluidic oscillation
Airlift bioreactor
COMSOL Mutiphysics

ABSTRACT

Airlift bioreactors can provide an attractive alternative to stirred tanks, particularly for bioprocesses with gaseous reactants or products. Frequently, however, they are susceptible to being limited by gas–liquid mass transfer and by poor mixing of the liquid phase, particularly when they are operating at high cell densities. In this work we use CFD modelling to show that microbubbles generated by fluidic oscillation can provide an effective, low energy means of achieving high interfacial area for mass transfer and improved liquid circulation for mixing.

The results show that when the diameter of the microbubbles exceeded 200 μm, the "downcomer" region, which is equivalent to about 60% of overall volume of the reactor, is free from gas bubbles. The results also demonstrate that the use of microbubbles not only increases surface area to volume ratio, but also increases mixing efficiency through increasing the liquid velocity circulation around the draft tube. In addition, the depth of downward penetration of the microbubbles into the downcomer increases with decreasing bubbles size due to a greater downward drag force compared to the buoyancy force. The simulated results indicate that the volume of dead zone increases as the height of diffuser location is increased. We therefore hypothesise that poor gas bubble distribution due to the improper location of the diffuser may have a markedly deleterious effect on the performance of the bioreactor used in this work.

1. Introduction

In spite of the accelerated development of bioreactors due to their widespread use, there are still difficulties in maintaining stability and rates of bioprocesses. It is believed that the most important causes of that failure have been poor construction and design, leading to inadequate mixing, which may jeopardize the

* Corresponding author at: Department of Chemical Engineering, College of Engineering, University of Baghdad, Baghdad, Iraq. Tel.: +964 0 7719069201.
E-mail address: mkh_control@yahoo.com (M.K.H. AL-Mashhadani).

http://dx.doi.org/10.1016/j.ces.2015.06.032

Nomenclature

Cd	viscous drag coefficient (dimensionless)
D	diameter of the bioreactor (m)
d	draught tube diameter (m)
d_b	bubble diameter (m)
g	gravity (m s^{-2})
hd	Height of gas sparger (m)
H	height of airlift bioreactor (m)
M_w	molecular weight of the gas bubble
m_{gl}	mass transfer rate (kg m^{-3} s^{-1})
R	ideal gas constant J (mol^{-1} K^{-1})
Re_b	Reynolds number (dimensionless)
P	pressure (Pa)
u_{slip}	relative velocity between two phases fluid (gas and liquid).
T	temperature of gas (K)
t	time (s)
u_l	velocity of liquid phase (m s^{-1})
u_g	velocity of gas phase (m s^{-1})
$\varnothing_l$	liquid volume fraction (m^3 m^{-3})
$\varnothing_g$	gas volume fraction (m^3 m^{-3})
ρ_l	density of liquid phase (Kg m^{-3})
ρ_g	density of gas phase (Kg m^{-3})
η_l	dynamic viscosity of liquid (Pa s)

Subscript

ALR	airlift bioreactor
CFD	Computational Fluid Dynamics

stability and performance of the process (Karim et al., 2005; Monteith and Stephenson, 1981; Karim et al. 2003).

Mixing in fermentation processes is required to prevent thermal stratification, maintain uniformity of the pH, increase the intimate contact between the feed and microbial culture, and prevent fouling and foaming. The importance of mixing in bioreactor design has encouraged numerous studies for many bioprocesses, including those producing biogas by anaerobic digestion (Stroot et al., 2001; Stafford, 2001; Bello-Mendoza and Sharratt, 1998).

Bello-Mendoza and Sharratt, 1998 concluded that the insufficient mixing can cause a remarkable decrease in both the efficiency of the fermentation process as well as the amount of biogas it produces. More importantly, efficient mixing can speed up reaction rates and therefore reduce the hydraulic retention times required (i.e. reduce the size of the reactor) or increase the throughput of medium (Monteith and Stephenson, 1981).

In bio-hydrogen production processes, for example, liquid mixing plays an important role according to Lay (2000, 2001). This author reported that the hydrogen produced from anaerobic fermentation of microcrystalline cellulose increased with increasing the agitation speed. Therefore, the mixing process in bioreactors is an important and critical factor in determining the efficiency of fermentation process and the nature of design which plays an active role in providing a suitable environment for micro-organisms.

The mechanism by which increased liquid circulation leads to improved reaction rates in three phase fermenter systems is due to it keeping cells and other solids in suspension (i.e. not settling out). This minimises resistance for mass transfer of dissolved non-gaseous species (nutrients, enzymes etc.) from the liquid phase to the surface of cells or solid substrates. It is highly likely that this effect, rather than improved gas transfer between bubble and bulk liquid is the most important explanation for the benefits of improved liquid circulation on fermenter performance. Indeed the work of Lewis and Davidson (1985) showed that there is no difference in gas–liquid mass transfer coefficient when the liquid velocity in an external loop reactor was doubled. i.e., K_L is constant with regard to the liquid velocity and the volumetric mass transfer coefficient K_La is only affected by gas void fraction and bubble size. It is generally recognized that K_L is a wake function of turbulence intensity and the work of Yawalkar et al. (2002) explains the effect of mixing and gas flow on gas–liquid mass transfer very well. However, the laminar regime and simulation used in the present paper is different from the turbulent bubble flows used by Lewis and Davidson (1985).

It should also be stressed that the major advance in micro-bubble injection into air-lift reactors (Zimmerman et al. 2009) is that the cloud of bubbles is injected with very low Reynolds numbers (10–100), just above the threshold for the onset of bubble formation. It was reported in that paper that microbubble clouds were generated with up to 18% less energy dissipation than steady flow, consistent with the observation that the onset pressure difference for bubble formation is ~20% less than steady flow with fluidic oscillation. In this low energy consumption regime, the boundary layer flow around the bubble is laminar and K_L is likely much lower than in conventional turbulent wakes.

Traditional mixing using stirred tanks may give better biogas yields but, when the process energy requirement is weighed against the extra energy obtained, these processes become economically unviable. Therefore, the reduction of the energy required for mixing is one the most challenging targets that is faced in large-scale bioenergy production.

The present study proposes the use of an airlift bioreactor as an alternative to stirred tanks for bioprocess applications. The airlift reactor (ALR) has been used in several industrial applications requiring gas–liquid contacting. ALRs can be classified into two main types: the external airlift loop reactor, in which the circulation takes place in separate conduits; and the internal airlift loop reactor, which is has a tube or a plate to create the conduit (channel) inside a single reactor for circulating the liquid inside the reactor (Chisti, 1989; Mudde and Van Den Akker, 2001) (Fig. 1).

In addition to good mixing, ALRs have long times for gas–liquid contacting and do not cause shear damage to cells. This has seen their widespread use in various biological processes, for example: biomass from yeast, vinegar, bacteria, etc. These advantages can be considerably further improved by equipping the ALRs with a fluidic oscillator for generating micro-bubbles which, compared to traditional stirred tanks, can dramatically increase the interfacial area between gas and liquid phases (Ying et al., 2014, 2013a, 2013b; Zimmerman et al., 2011a, 2011b).

2. Micro-bubble generated by fluid oscillation

Traditionally, enhancement of mass and heat transfer rates in gas–liquid contacting have always been accomplished by increasing the interfacial area between gas and liquid phases. Due to their high maintenance cost and energy requirements, use of traditional methods (e.g. stirred tanks) to achieve certain preset goals is not economically convincing. However, this scenario could be changed if microbubbles systems are used in chemical and biochemical processes. These systems would make dramatic improvements to mass flux by increasing surface-area-to volume ratios of a bubble.

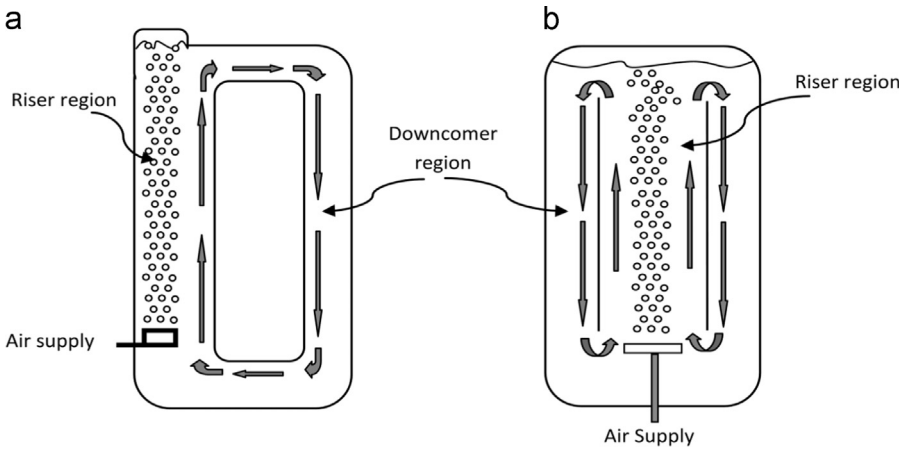

Fig. 1. Schematic of airlift bioreactor with (a) external recirculation and (b) internal recirculation.

Fig. 2. Microbubbles generated by fluidic oscillation, and fine bubble without fluidic oscillation.

However, the use of small bubbles increases the height of the foam, which is undesirable characteristic in many applications (Seetharaman et al., 2014; Zayas, 1997; Stevenson and Li, 2014; Prud'homme and Khan, 1996).

In spite of the successive developments of microbubble generation systems, the energy requirements are still reasonably high. Zimmerman et al. (2009, 2011a, 2011b) have developed a novel aeration system by fluidic oscillation, which is capable of producing gas bubbles with micron size to achieve enhanced heat and mass transfer rates. As well as, increased interfacial area, microbubbles offer hydrodynamic stabilisation, longer residence times and an increased mixing efficiency. The fluidic oscillation method has low energy demands compared to other methods for microbubble generation.

The essential idea of this novel system is to use oscillatory flow to interrupt the air flow and limit the time available for growth of the bubbles as shown in Fig. 2. The oscillation frequency can be easily adjusted by changing the feedback loop length in order to create bubbles of the required size when the outputs are fed to separate diffusers as shown in Fig. 3. AL-Mashhadani et al. (2012) used this technology for stripping carbon dioxide. They reported that the efficiency of CO_2 stripping was about 29% more than that for fine bubble sparging. There is a far greater uniformity of spacing and bubble size distribution with jet diversion fluidic oscillation than with steady flow, which allows the fundamental assumption of the two fluid bubbly flow model- uniformly sized and homogeneously dispersed microbubbles. Fluidic oscillation for bubble generation can give quite a narrow size distribution, visually supported in Fig. 2, to support this modelling idealisation.

3. Airlift bioreactor design and simulation

Bioreactors are influenced by the complexity of the biological medium. This is generally a multiphase solution consisting of cells and nutrients in solid, liquid and gas forms. A fundamental understanding of bioreactor flow mixing patterns helps to provide optimal conditions for growth and product formation when assisted by reliable control systems for pH and temperature monitoring. There are many possible shape options of the bioreactor configuration, which depend on several parameters (e.g. efficiency of mixing, cost etc.). Cylindrical is a conventional German design and egg-shaped configurations have been widely used in the world, whereas rectangular cross-section reactors have more limited uses due to poorer mixing efficiency (Metcalf and Eddy, 2003). Cylindrical bioreactor with airlift gas injection was modelled in the current simulation study. This bioreactor is currently being used in studies of microbubble-enhanced anaerobic digestion. The diameter of the draught tube to bioreactor diameter ratio (d/D) is 0.6 and the angle of the conical bottom is 25°. The total volume of the reactor is 15 l with a working volume of 8–9 l. The remaining volume of the bioreactor is used as headspace volume, which is necessary to condense the vapour water and return it to the medium as shown in Fig. 4.

The biological medium in a working bioreactor is typically opaque slurry containing organic materials, solids, bacteria, dispersed gas bubbles. It is difficult to visibly see the efficiency in the mixing process even when using high-speed cameras. Computer simulation provides a powerful means for optimising bioreactor design for two reasons. Firstly, for a specific bioreactor configuration such as that described above, it enables the internal flow patterns to be mapped to a level of precision that is beyond experimental techniques. Secondly, it allows the effect of key design decisions on overall bioreactor performance to be rapidly evaluated in silico. Computational Fluid Dynamics (CFD) software is increasingly being deployed to simulate, trouble-shoot and design bioreactors.

Previous work on anaerobic digestion has led to this more general work on the simulation of airlift bioreactors presented

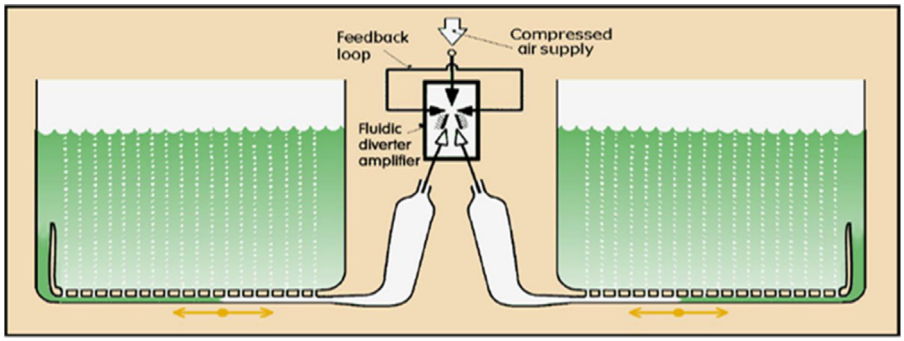

Fig. 3. Fluidic oscillator system for microbubble generation. Each oscillating output is connected to a diffuser and the rapid interruptions in gas flow in each result in bubble diameters of the order of the aperture diameter.

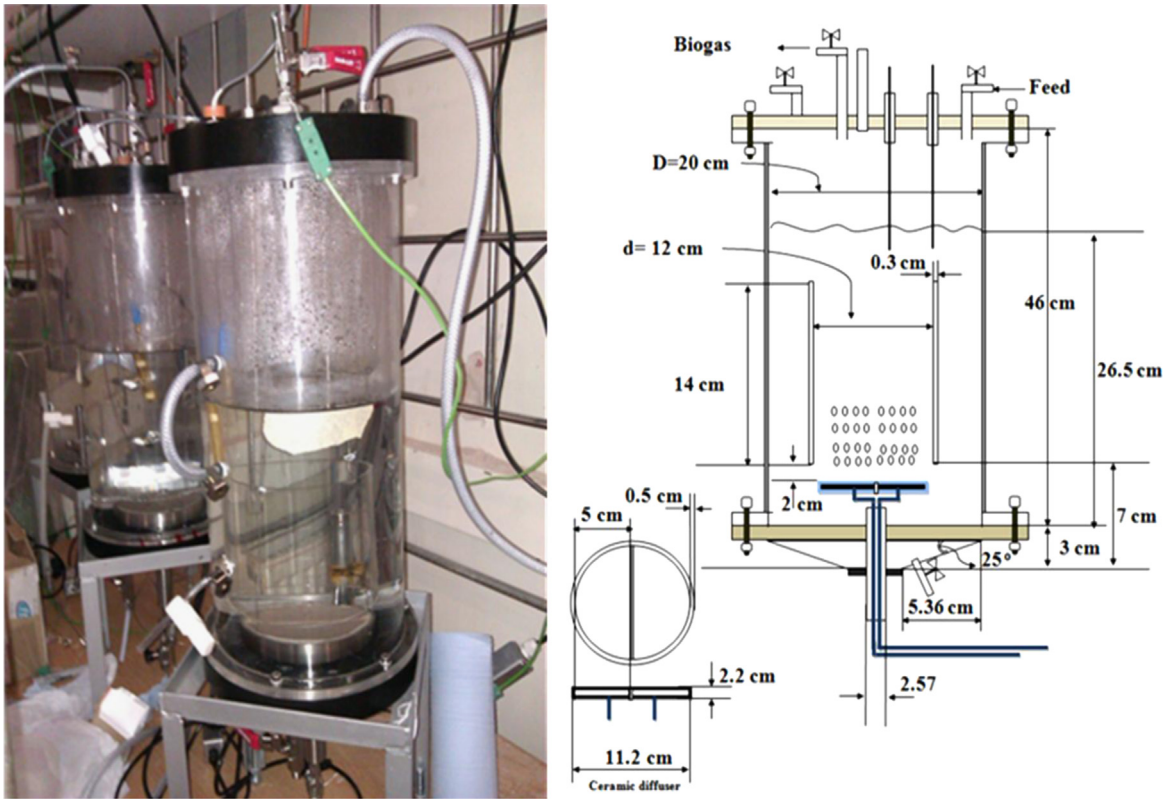

Fig. 4. Airlift bioreactor modelled in this study with diagram showing its dimensions.

here. Other researchers have used simulation to contribute to the development and design of the bioreactors. These authors include, Vesvikar and Al-Dahhan (2005), Wu and Chen (2008), Meroney and Colorado (2009), Wu (2009), (2010), Terashima et al. (2009), Oey et al. (2001), Šimčík et al. (2011), Becker et al. (1994), Calvo (1989), Calvo and Leton (1991) and Moraveji et al. (2011). CFD has been used in two ways: firstly to improve the performance of the mixing regime in the reactor and, secondly, to investigate the effect of an existing design on the efficiency of bioprocess. Meroney and Colorado (2009), studied the impact of changing dimensions of the mixing parts on the efficiency of mixing in the digester.

In a different study, Wu (2009), has used many different types of mixing methods in order to identify the effect of each of these on the performance of the bioprocess. Wu and Chen (2008), and Vesvikar and Al-Dahhan (2005) have developed a design of a mixing system and have tested all the variables that would lead to a higher efficiency of the developed system in the anaerobic digester using CFD software. Huang et al. (2010) studied the hydrodynamic and local mass transfer in the airlift bioreactor. The authors mentioned that the mass transfer rate in the riser region is higher than any other region of the reactor. In the current study, COMSOL Multiphysic software (version 4.1) was used, which is considered an efficient way to evaluate and describe the flow dynamic in airlift bioreactors. The gas holdup and liquid velocity are investigated in the present study as a main flow dynamic parameter (Calvo et al. 1991).

4. Flow modelling of the airlift bioreactor

A simulation process of the airlift bioreactor was carried out using COMSOL Multiphysics software (Version 4.1). The airlift bioreactor configuration that was used in the simulation is illustrated in Fig. 4. The present study used a range of microbubble diameters between 20 and 1000 μm with low gas (air) concentration in water as a liquid phase. The temperature and pressure in this modelling were 298.15 K and 1 atm respectively.

A laminar bubbly flow model interface was used for modelling of the two-fluid flow regimes (e.g. mixture from gas bubbles and liquid). Thus, the momentum transport equation is given by:

$$\varnothing_l \rho_l \frac{\partial u_l}{\partial t} + \varnothing_l \rho_l u_l . \nabla u_l = -\nabla P + \nabla . \left[\varnothing_l \eta_l \left(\nabla u_l + \nabla u_l^{T} \right) \right] + \varnothing_l \rho_l g \quad (1)$$

where $\varnothing_l$ is liquid volume fraction (m^3/m^3), ρ_l is density of liquid, u_l the velocity of liquid phase (m/s), t is time (sec), P is pressure (Pa), η_l is dynamic viscosity of liquid phase (Pa s) and g the gravity (m/s^2).

For low gas concentrations, the liquid holdup coefficient ($\varnothing_l$) is approximately one. Therefore, the change of $\varnothing_l$ can be neglected in the following equation:

$$\frac{\partial \varnothing_l}{dt} + \nabla . (\varnothing_l u_l) = 0$$
$$\nabla . u_l = 0 \quad (2)$$

The momentum transport equation for the gas phase is illustrated as follows:

$$\frac{\partial \rho_g \varnothing_g}{\partial t} + \nabla . \left(\varnothing_g \rho_g u_g \right) = -m_{gl} \quad (3)$$

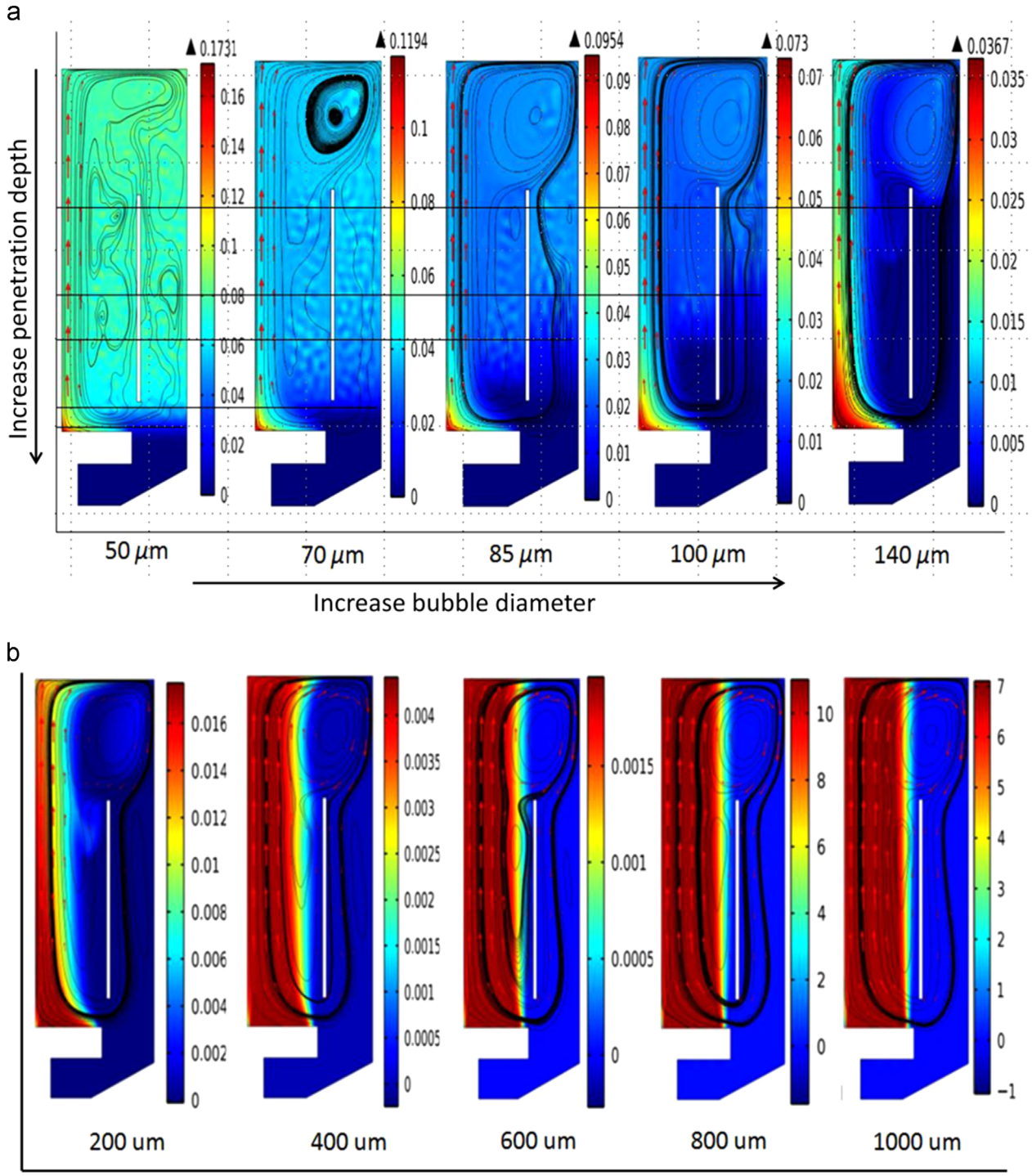

Fig. 5. Snapshots of gas concentration at different bubble diameter after steady state (a) bubble diameter 50, 70, 85, 100 and 140 μm (b) bubble diameter 200, 400, 600, 800 and 1000 μm.

where ρ_g is the density of gas phase (kg/m^3), $\varnothing_g$ gas volume fraction (m^3/m^3), u_g is velocity of gas and $-m_{gl}$ the mass transfer rate (kg/m^3/s).

As the approximation of the present paper, there is no mass transfer between gas and liquid phases. Thus $m_{gl}=0$. Therefore, the continuity equation can be arranged for two phases (e.g. gas and liquid) but without mass-transfer terms as follows:

$$\frac{\partial \rho_g \varnothing_g}{\partial t}+\nabla.\left(\varnothing_g \rho_g u_g\right)=0 \tag{4}$$

The ideal gas law was used to calculate the density of gas (ρ_g)

$$\rho_g=\frac{P\,M_w}{RT} \tag{5}$$

where M_w is the molecular weight of the gas bubble, R is the ideal gas constant (8.314 J/mol/K) and T the temperature of gas (K).

The gas volume fraction is estimated by the following equation:

$$\varnothing_g=1-\varnothing_l \tag{6}$$

The gas velocity can be determined as $u_g=u_l+u_{slip}$, since u_{slip} is relative velocity between two-phases fluid (gas and liquid).

Pressure-drag balance, obtained from slip model, was used to calculate u_{slip}. The assumption of this model suggests that there is a balance between viscous drag and pressure forces on the gas microbubble:

$$\frac{3Cd}{4d_b}\rho_l|u_{slip}|u_{slip}=-\nabla P \tag{7}$$

where Cd is the viscous drag coefficient (dimensionless), d_b is bubble diameter (m). Owing that the microbubble diameters used in the simulation are equal or less than 1000 μm, the Hadamard–Rybczynski drag law was used, and hence:

$$\mathrm{Cd}=\frac{16}{Re_b} \tag{8}$$

where:

$$Re_b=\frac{d_b\rho_l|u_{slip}|}{\eta_l} \tag{9}$$

where Re_b is Reynolds number.

Two dimensions model with axial – symmetry has used to model the airlift bioreactor in the current study. On the draft tube and internal airlift bioreactor walls, no slip ($u=0$) was used in boundary conditions (BCs) for liquid phase, whilst no gas flux values were used for the gas bubble phase, hence the values of u_l and $n(u_g\varnothing_g)$ equal to zero. In the other hand, the "gas outlet" and the slip ($n.u=0$) BCs were used at the top of liquid phase for both liquid phase and gas phase, respectively. The pressure point constraint of the upper right corner equals to zero. On the top of the diffuser, no slip boundary conditions were used for liquid phase and the "gas flux" boundary conditions for the gas phase.

A mesh resolution study was conducted with a base case of an extra fine mesh with 2141 elements. Doubling the elements did not affect dramatically the calculation of the reported variables especially for bubbles 200 microns and larger. The trends remain the same for all reported variables, so mesh resolution does not influence generalizations drawn from the results.

5. Results and discussion of simulation study

The distribution of gas volume fraction and the liquid velocity streamlines at different bubble diameters (50, 70, 85, 100, 140, 200, 400, 600, 800 and 1000 μm) are presented in Fig. 5. The simulation time required for each run to achieve steady state increased with decreasing bubble size as can be seen in this figure. The 50 μm bubble simulation had reached a steady state in around 900 s.

It can be observed in Fig. 5 that gas bubbles are not present in the downcomer for bubble sizes of 200 μm or greater (i.e. the volume gas fraction is zero in this region of the reactor). However, in simulations using bubble diameters of 50 μm and 100 μm, there is recirculation of gas bubbles in the downcomer in which the steady state volume gas fractions are 0.08 and 0.01 respectively as shown in Fig. 6, which illustrate the effect of smaller bubble sizes on the simulation convergence to steady state. For bubbles exceeding 200 μm, therefore, both mass and heat transfer are confined to the riser region, because the downcomer region, which is equivalent to more than 60% of overall working volume of the reactor is free of gas bubbles. The liquid circulation is unable to overcome the higher buoyancy of bigger bubbles so they no longer circulate.

However, as just discussed, this situation is different for bubbles that are 100 μm or smaller. For example, for a bubble diameter of 50 μm, the volume gas fraction of 0.075 is extremely high compared to other experimental work in similar airlift reactors using larger bubble sizes such as results reported by Rengel et al. (2012). These authors give a maximum downcomer volume fraction of around 0.045 but to achieve this they require a superficial gas velocity of 0.047 m/s which is two orders of magnitude greater than that used in this work (0.00044 m/s). This gives an indication of the huge benefits in mass transfer performance that microbubbles can achieve. However, this can be disadvantageous if gas throughput is a system objective. For instance, if 4.7 m³/s gas flow rate is to be processed, a bubble column with a cross-sectional area of diameter of 100 m^2 (11 m), while with microbubble reactor, the cross sectional area will be 10,682 m² (diameter of 116.6 m).

To put it another way, a volume gas fraction of 0.075 corresponds to an enormously high interfacial area of 9000 m^2/m^3 which is around three orders of magnitude greater than experimental values reported for typical bubble columns using standard bubble sizes of a few millimetres (Maceiras et al., 2010). In addition, Calvo (1989) mentioned that the gas hold up in the riser region increases with increasing gas flow rate. Thus, a large volume of gas is lost leading to poor processing efficiency and suboptimal economy. But, the present study demonstrates that the gas fraction in both regions of reactor (riser region and downcomer region) can be achieved, but with much lower gas inflow, if the microbubble technology is used in the sparging system.

Note that an accurate experimental validation of the potentially huge increase in interfacial areas is challenging since it would require the production of a monodisperse swarm of very small microbubbles of 50 μm. This is still beyond the scope of current implementations of the fluidic oscillator despite the smaller sizes and narrower distributions which it is capable of delivering

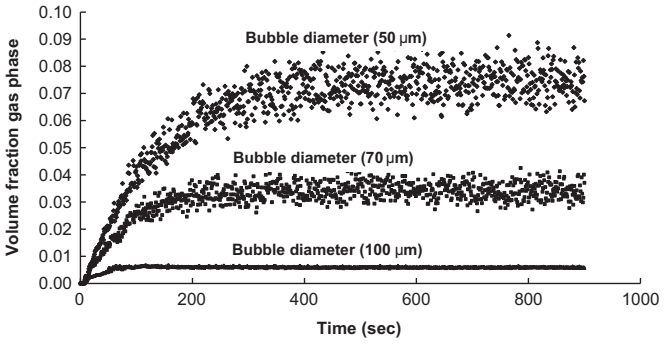

Fig. 6. Dynamic evolution of average simulated gas phase volume fraction in the downcomer for smaller bubble sizes (50, 70, and 100 μm).

compared to standard sparging systems. In addition, our model ignores bubble coalescence which is likely to be a dominating factor as the voidage, and hence the number of bubble collisions, increases. The aim of this work, however, is to demonstrate the direction of travel suggested by the model; that very high interfacial areas might be possible if bubbles smaller than 70 μm can be reliably produced. The model shows that increased gas recirculation gives higher bubble residence times that strongly increase the interfacial area at these small bubble sizes.

It should also be noted that the presence of bubbles in the downcomer region for the smaller bubble sizes allows significant mass transfer to occur in this region. Furthermore, the higher rates of gas recirculation give longer gas residence times and so, along with the higher interfacial area, provides even further benefits for gas–liquid mass transfer. Experimentally, we have observed the presence of micro-bubbles generated by fluidic oscillation in the downcomer, and the disappearance of these bubbles when the oscillator is turned off (increasing bubble size). However, the overall reaction kinetics and mass transfer play an important role in limiting these advantages. For example, for fast reactions, the reactive gas in the bubbles would have already depleted by the time they rise to the top the riser, thus recycling them back into the downcomer does not benefit the mass transfer. On the contrary, those bubbles just occupy the working volume of the reactor and displace the liquid medium.

6. Liquid and gas velocity profile

Fig. 7 shows, for different bubble sizes, the gas velocity profiles across the radius of the riser zone at a level of 0.12 m from the bottom of the reactor. Fig. 8 shows the centreline gas velocities in the Y (vertical) direction in the riser zone. The simulation data shows that at this low gas flow rate (300 ml/min), the gas velocity decreases with decreasing bubble size, as would be expected, due to the increased drag force. The corresponding liquid velocity profiles are shown in Figs. 9 and 10 that show that the liquid velocity increases with decreasing bubble size for bubbles larger than 100 μm. This is to be expected due increased momentum transfer between gas and liquid for smaller bubbles. Although the naïve observer conclude that larger, faster rising bubbles might generate more turbulence and better liquid mixing, this is localised to the immediate vicinity of the bubbles. Smaller, slower moving bubbles, on the other hand, do a better job at dragging the liquid along with them, thereby generating stronger liquid circulation and better mixing throughout the reactor.

Fig. 10 shows also that the liquid velocity decreases when the bubbles diameter decrease less than 100 μm. Indeed, when the sparging started, the liquid velocity for 50 μm bubbles was larger than liquid velocity for 100 μm bubbles. This behaviour changed,

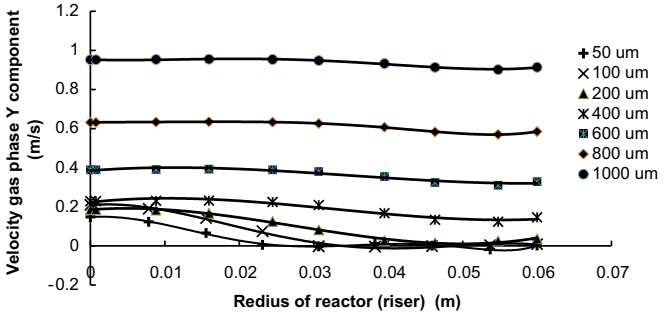

Fig. 7. Velocity gas profile (Y-component) in cross-section riser zone after steady state at different gas bubble diameter (50,100, 200, 400, 600, 800, 1000 μm) after steady state.

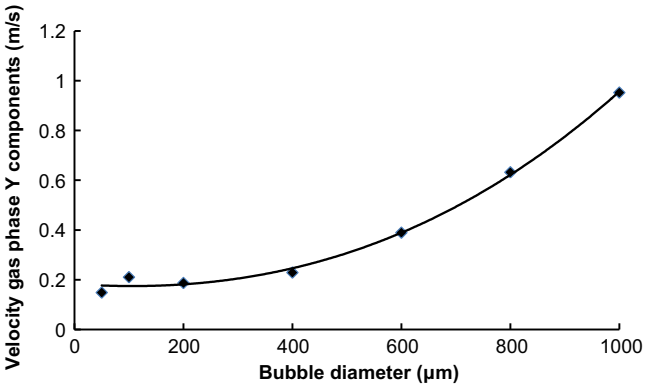

Fig. 8. Velocity profile in certain point riser zone after steady state.

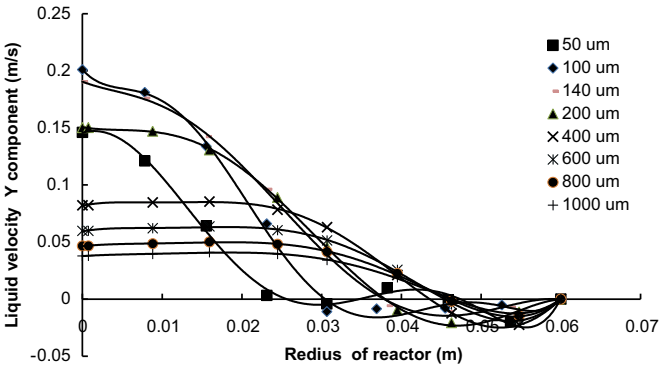

Fig. 9. Velocity liquid profile in cross-section riser zone after steady state at different gas bubble diameter (50,100,140, 200, 400, 600, 800, 1000 μm) after steady state.

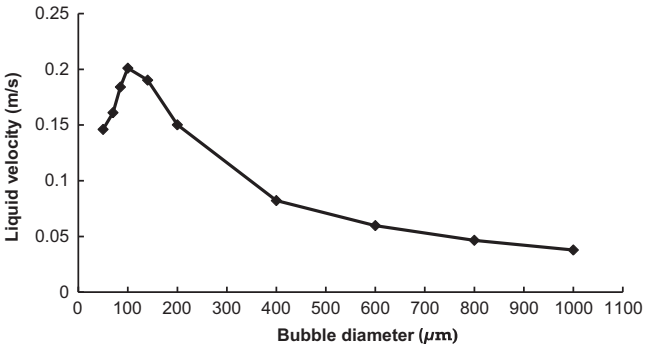

Fig. 10. Velocity profile of liquid phase in certain point in riser zone after steady state.

since the liquid velocity for 50 μm bubbles decreases with time by 25% to become less than its velocity when diameter of bubble is 100 μm. It can be also noticed that this unexpected decrease in liquid velocity in riser region (for 50 μm bubbles) has occurred when the gas concentration increased in downcomer region, as can be seen in Fig. 11. Hence, these results indicates that the presence of high concentration of microbubbles in downcomer region obstruct the recirculation of the liquid around the draft tube in the bioreactor due to increasing buoyancy force in that area (downcomer region).

The simulations show a fivefold increase in centreline liquid velocity for 100 μm bubbles as compared to 1000 μm bubbles for the same gas flow rates. Micro-bubbles, therefore, are able to move the liquid quite rapidly upwards even at low gas flow rates. The fact that micro-bubbles can provide strong liquid circulation at very low gas flow rates shows that they could give a very big

reduction in the energy required to provide adequate mixing in bioreactors.

It is interesting to see the appearance of negative liquid velocities (i.e. downward flow) in increasingly large portions on the outer edge of the riser for smaller bubbles sizes (Fig. 8). A comparison, for example, of the 100 μm and the 200 μm bubbles suggests that the former are, owing to their reduced slip velocity, concentrated into a more focussed column by the returning liquid circulating from the downcomer. These results in the formation of large circulating eddy in the riser for smaller bubble sizes as can be seen in Fig. 5.

7. Effect of bubble size and diffuser positioning on microbubble penetration and dead zones

The penetration depth of micro-bubbles into the downcomer zone was also investigated in the present study. The depth of penetration influences the rate of heat and mass transfer in the reactor since it effects the overall residence time of gas bubbles in the reactor and also the total interfacial area. The simulation data shows that the depth of penetration of the microbubbles increases with decreasing bubble size. Fig. 12 presents the gas volume fraction profiled in the downcomer region for various bubble diameters (50, 70, 85, 100 and 140 μm). The Figure clearly demonstrates the origin of the horizontal lines in Fig. 5 (a) respectively from lowest to highest. The position of the gas diffuser in the reactor is an important design factor since, like bubble size, it also influences gas penetration in the downcomer. The airlift bioreactor was simulated with four different locations of gas sparger. The ratio of height of gas sparger to height of airlift bioreactor (hd/*H*) was varied from 0.17 to 0.37. Figs. 13 and 14 show that with similar bubbles diameter (i.e. 50 μm), the deeper penetration could be achieved at a lower (hd/*H*). Note that, in this study, the effect of varying the diffuser location (a key reactor design parameter) gives results that are entirely to be expected, i.e. the extent of bubble penetration in the downcomer remains fixed when measured relative to the diffuser position.

In some of bioprocesses, for example; anaerobic digestion process, the sludge contains a soot, dust, heavy metals and suspended matter, which affect the fermentation efficiency and blocks the porous of diffuser. In the current study, the settling velocity of these impurities has taken into consideration with designing this bioreactor to avoid these problems as well as cleaning purposes. Therefore, the hd/*H* ratio of 0.17 has been found as the best position to mount diffusers in airlift digester.

The fluid is essentially stagnant below the diffuser and therefore a higher positioning of the diffuser has a predictable effect on the size of this dead zone as illustrated in Fig. 15 which shows the steady state distribution of gas concentration in the reactor at various diffuser positions (0.05, 0.065, 0.08, 0.095, 0.11 m above the bottom of the reactor) for the 50 μm bubble size. The results confirm that, for each diffuser position, there is negligible gas volume fraction and liquid circulation below the level of the diffuser. This region can therefore be considered to be a dead zone. Although in general, dead zones are to be avoided a practical consideration in anaerobic digesters in the settling of solids directly on the sparger surface that can inhibit its performance. This is the reason that the experimental bioreactor discussed in this section has the diffuser at a slightly elevated level of 0.05 m above the reactor bottom (hd/*H*=0.17). The simulation results therefore confirm that improper location of the diffuser can give poor bubble distribution and may have a deleterious effect on the

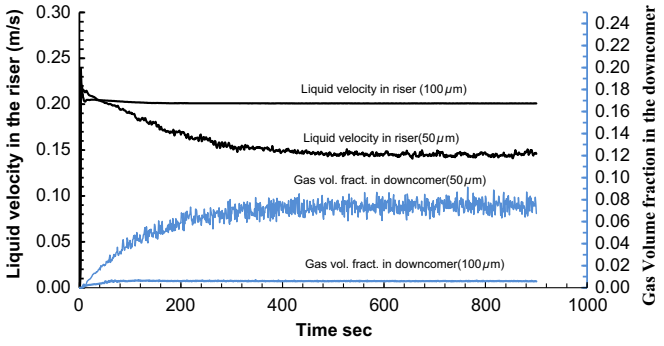

Fig. 11. Liquid velocity in riser region and gas volume fraction in downcomer region for 50 μm and 100 μm bubble diameter after steady state. It can be seen that the velocities of liquid on left side of chart, while gas velocity on right side of the chart.

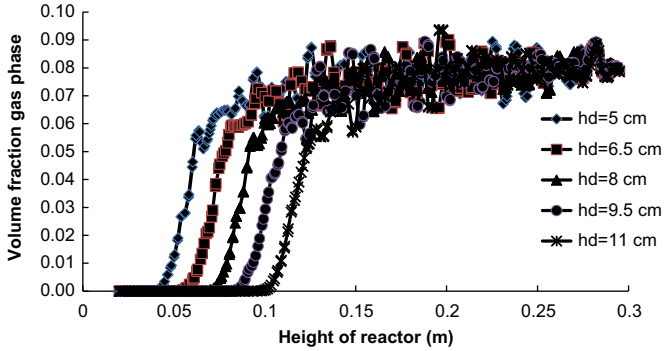

Fig. 13. Volume gas fraction with height of airlift digester at different diffuser position (5,6.5, 8,9.5,11 cm) at 50 μm and after steady state.

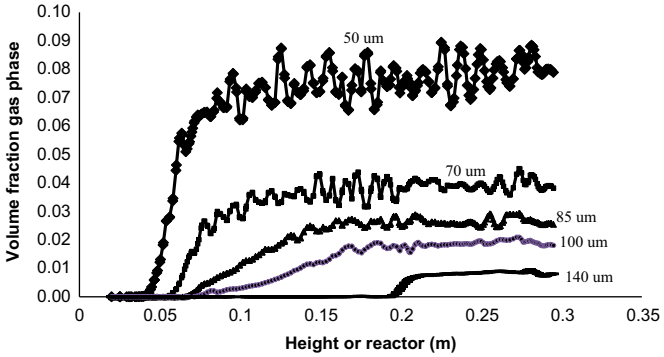

Fig. 12. Gas volume fraction versus height above bottom of reactor in the downcomer for (50, 70, 85, 100, 140 μm) after steady state. Note that the diffuser position for these simulations is 0.05 m above the bottom of the reactor.

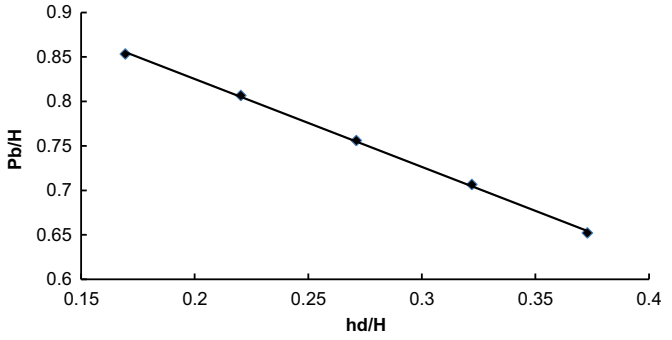

Fig. 14. Height of diffuser and height of reactor ratio (hd/*H*) with height of penetration and height of reactor ratio (Pb/*H*) at micro-bubble diameter of 50 μm.

performance of anaerobic digester. It should also be noted, however, that dead zones are often designed into reactors on purpose specifically for the removal of sediment at the bottom of the reactor. In this case the results indicate that a dead zone (i.e. negligible gas penetration and liquid mixing) of arbitrary height can be easily created by simple by adjustment of diffuser position.

8. Effect of draft tube diameter

Since the relative flow area of the riser compared to the downcomer is an important design parameter for internal airlift reactors, we simulated four different draft tube diameters. The ratio of draft tube diameter to the bioreactor diameter (d/D) was varied from 0.6 to 0.9. Two bubble diameters (50 μm and 400 μm) were used for investigating effect the draft parameter on mixing efficiency. Fig. 16 shows the liquid circulation patterns and the steady state distribution of gas volume fraction for d/D=0.6, 0.7, 0.8, and 0.9, when the bubble diameter is 400 μm, while Fig. 17 shows the corresponding velocity liquid profiles across the cross section of the riser region. An interesting aspect of these results is that the liquid circulation in the downcomer is very low for the largest riser diameters (d/D=0.8 and 0.9) with most liquid circulating downwards in the riser. The reactor is therefore

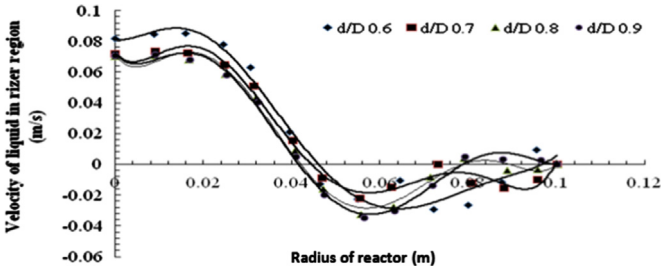

Fig. 17. Velocity liquid profile in cross-section after steady state.

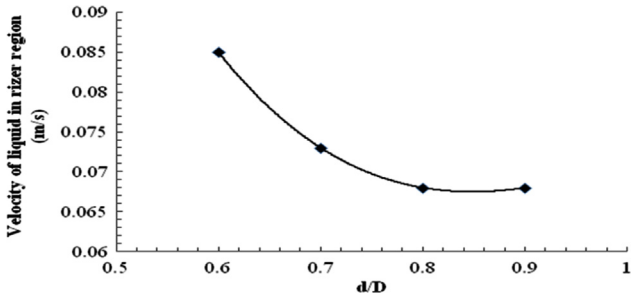

Fig. 18. Velocity liquid in cross-section riser region at different draft tube diameter after steady state.

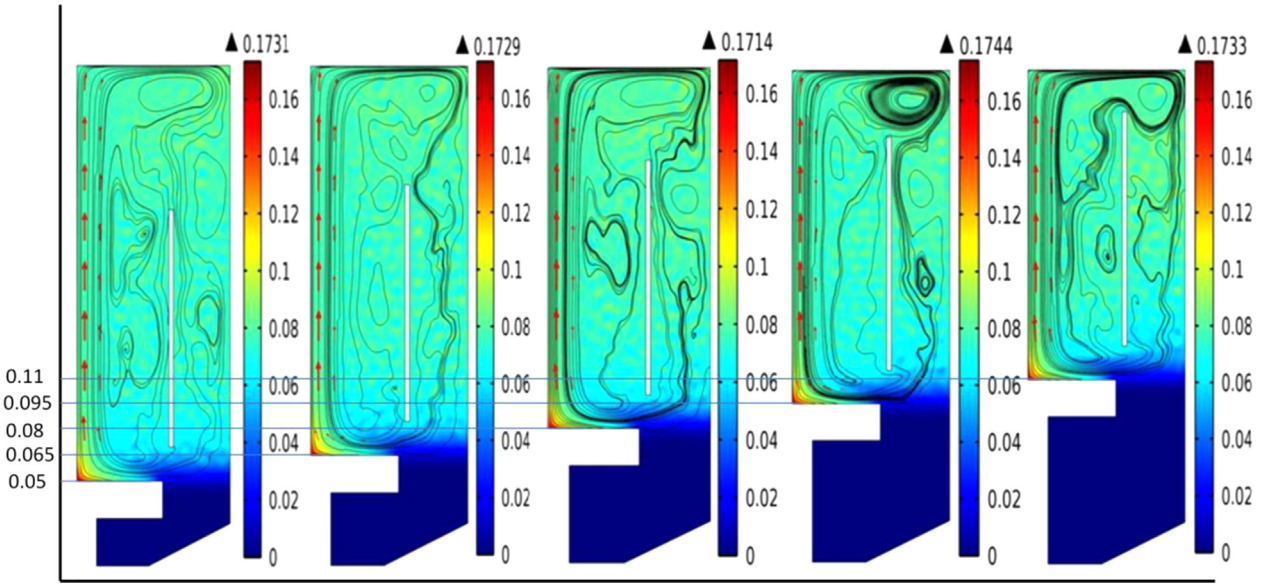

Fig. 15. Snapshots of gas concentration after steady state condition different diffuser position (0.05, 0.065, 0.08, 0.095, 0.11 m).

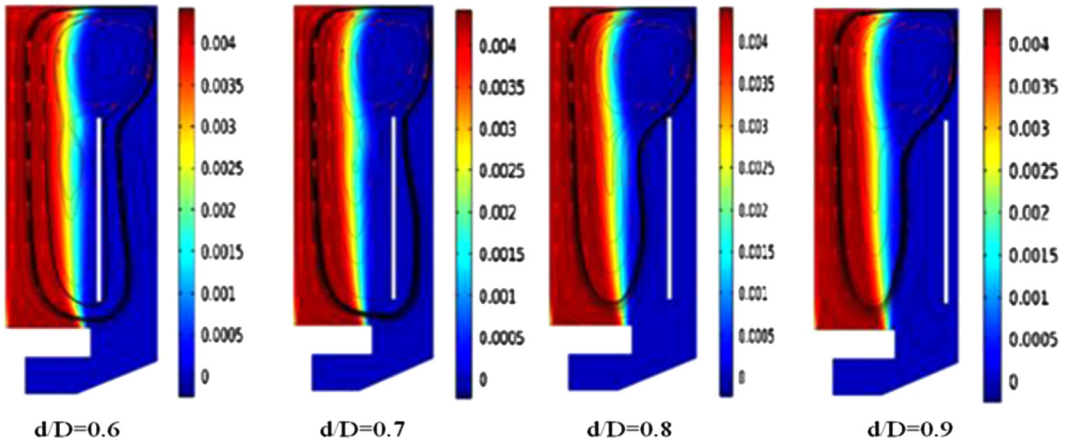

Fig. 16. Snapshots of gas concentration at different d/D (d/D=0.6, 0.7, 0.8, and 0.9) when microbubble diameter is 400 μm after steady state.

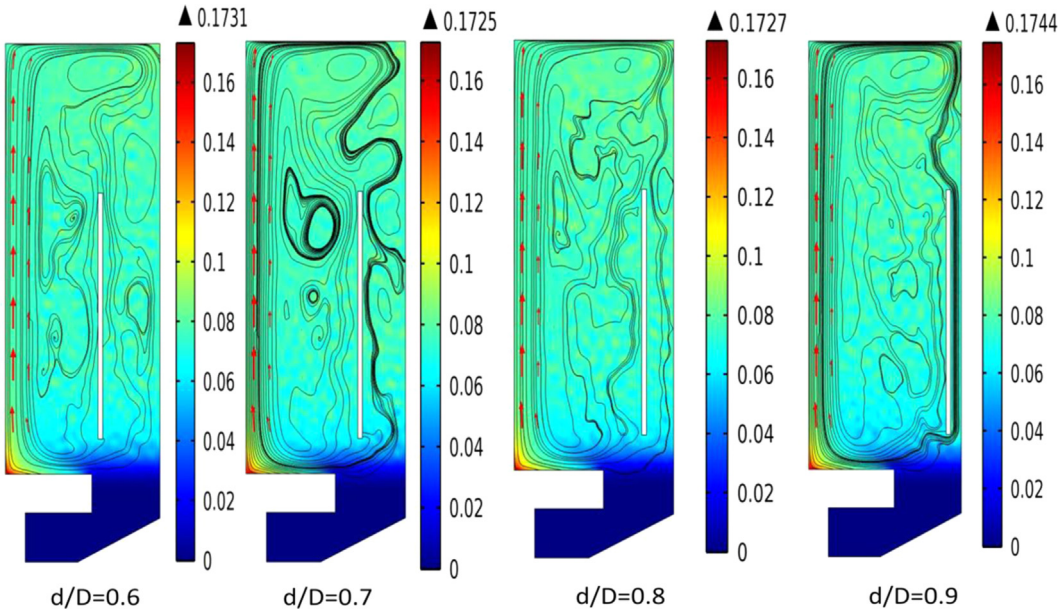

Fig. 19. Snapshots of gas concentration at different d/D (d/D=0.6, 0.7, 0.8, and 0.9) when microbubble diameter is 50 μm and after steady state.

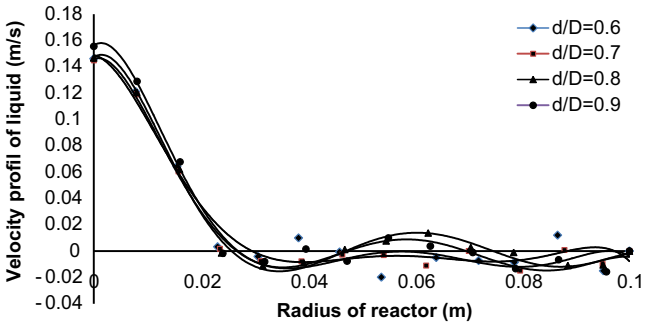

Fig. 20. Velocity liquid profile in cross-section after steady state.

operating as a simple bubble column in these simulations. Indeed, for d/D=0.8 and 0.9, it can be seen in Fig. 18, that this stagnant region extends beyond the downcomer well into the riser. Our simulation results therefore show a marked transition from a liquid circulation pattern that has good mixing for d/D=0.6, to one that has a large annular dead zone of poorly mixed liquid.

In order to assess the effect of much smaller microbubbles size, simulations were performed for the 50 μm bubble size and the results are shown in Figs. 19 and 20. It can be seen that the increase in draft tube diameter has very little effect on the liquid velocity profile (Fig. 20) but may causes slightly more swirling flow in the reactor (Fig. 19).

9. Conclusions

Understanding and optimising the efficiency of mixing and mass transfer is a key concern in many bioprocess applications including those that use airlift bioreactors. Aeration remains a key concern and cost factor in many processes and even anaerobic processes such as biogas production can be significantly enhanced by better gas–liquid mass transfer. The design and simulation of an airlift bioreactor with aeration using microbubbles generated by fluidic oscillation has been addressed in the present study. This is the first simulation study to comprehensively analyse the effect of microbubbles on mixing and transport in airlift reactors. The results show that the use of microbubbles of 50 μm diameter can dramatically increase the interfacial area available for mass transfer and also the residence time of the gas bubbles. This is due to much higher levels of gas recirculation for microbubbles when compared to larger bubbles. In addition, the results also show that, for the low gas flow rate studied (300 ml/min), microbubbles increase the liquid circulation velocity and therefore give the potential for better mixing.

Finally, we used the simulations to investigate key design decisions on the geometry of the bioreactor: the vertical positioning of the diffuser and the draft tube diameter in order to avoid dead zones of poor mixing and mass transfer. Overall, the results obtained suggest enormous potential for microbubble aeration for improving the efficiency of mixing and mass transfer. They also demonstrate the power of computational modelling for the analysis and design of the next generation airlift bioreactors for bioprocess applications.

Acknowledgement

W.Z. would like to acknowledge support from the EPSRC (Grant no. EP/I019790/1 and EP/K001329/1). W.Z. would like to acknowledge the Royal Society (UoS No. 127438) for a Brian Mercer Innovation award and the Royal Academy of Engineering for an industrial secondment with AECOM Design Build. MKHaM would like to thank Ministry of Higher Education and Scientific Research in Iraq and University of Baghdad for a doctoral scholarship (Ministerial order No. 17073). S.W. would like to acknowledge support from MWH UK. The authors would like to acknowledge the support of Dr. Hemaka Bandalusena (Loughborough University, UK). The Authors would like to thank the referee for deep insight into bubbly flow dynamics and benefit of his experience.

References

AL-Mashhadani, M.K.H, Bandalusena, H.C.H., Zimmerman, W.B., 2012. CO2 mass transfer induced through an airlift loop by a microbubble cloud generated by fluidic oscillation. Ind. Eng. Chem. Res. 51 (4), 1864–1877.

Becker, S., Sokolichin, A., Eigenberger, G., 1994. Gas–liquid flow in bubble columns and loop reactors: Part II. Comparison of detailed experiments and flow simulations. Chem. Eng. Sci. 49, 5747–5762.

Bello-Mendoza, R., Sharratt, P.N., 1998. Modelling the effects of imperfect mixing on the performance of anaerobic reactors for sewage sludge treatment. J. Chem. Technol. Biotechnol. 71, 121–130.

Calvo, E.G., Letón, P., 1991. A fluid dynamic model for bubble columns and airlift reactors. Chem. Eng. Sci. 46, 2947–2951.

Calvo, E.G., 1989. A fluid dynamic model for airlift loop reactors. Chem. Eng. Sci. 44, 321–323.
Calvo, E.G., Letón, P., Arranz, M.A., 1991. Prediction of gas hold up and liquid velocity in airlift loop reactors containing highly viscous Newtonian liquids. Chem. Eng. Sci. 46, 2951–2954.
Chisti, M.Y., 1989. Airlift Bioreactor. Elsevier Applied Science, London, UK.
Huang, Q., Yang, C., YU, G., Mao, Z.-S., 2010. CFD simulation of hydrodynamics and mass transfer in an internal airlift loop reactor using a steady two-fluid model. Chem. Eng. Sci. 65, 5527–5536.
Karim, K., Haffmann, R., Klasson, K.T., Al-Dahhan, M.H., 2005. Anaerobic digestion of animal waste: effect of mode of mixing. Water Res. 30 (15), 3597–3606.
Karim, K., Klasson, K.T., Hoffmann, R., Dresher, S.R., Depaoi, D.W., Al-Dahhan, H., 2003. Anaerobic digestion of animal waste: effect of mixing. Energ. Environ-UK 7 (359), 175–185.
Lay, J.-J., 2000. Modeling and optimization of anaerobic digested sludge converting starch to hydrogen. Biotechnol. Bioeng. 68, 269–278.
Lay, J.-J., 2001. Biohydrogen generation by mesophilic anaerobic fermentation of microcrystalline cellulose. Biotechnol. Bioeng. 74, 280–287.
Lewis, D.A., Davidson, J.F., 1985. Mass transfer in a recirculating bubble column. Chem. Eng. Sci. 40 (11), 2013–2017.
Maceiras, R., Álvarez, E., Cancela, M.A., 2010. Experimental interfacial area measurements in a bubble column. Chem. Eng. J. 163, 331–336.
Meroney, R.N., Colorado, P.E., 2009. CFD simulation of mechanical draft tube mixing in anaerobic digester tanks. Water Res. 43 (4), 1040–1050.
Metcalf, Eddy, 2003. Wastewater Engineering Treatment And Reuse. McGraw Hill, New York, USA.
Monteith, H.D., Stephenson, J.P., 1981. Mixing efficiencies in full-scale anaerobic digesters by tracer methods. Water Pollut. Control Fed. 53 (1), 78–84.
Moraveji, M.K., Sajjadi, B., Jafarkhani, M., Davarnejad, R., 2011. Experimental investigation and CFD simulation of turbulence effect on hydrodynamic and mass transfer in a packed bed airlift internal loop reactor. Int. Commun. Heat Mass 38, 518–524.
Mudde, R.F., Van Den Akker, H.E.A., 2001. 2D and 3D simulations of an internal airlift loop reactor on the basis of a two-fluid model. Chem. Eng. Sci. 56, 6351–6358.
Oey, R.S., Mudde, R.F., Portela, L.M., Van Den Akker, H.E.A., 2001. Simulation of a slurry airlift using a two-fluid model. Chem. Eng. Sci. 56, 673–681.
Prud'homme, R.K., Khan, S.A., 1996. Foams, theory, measurements, and applications. Surfactant Sci. Ser. 57, 146–151.
Rengel, A., Zoughaib, A., Dron, D., Clodic, D., 2012. Hydrodynamic study of an internal airlift reactor for microalgae culture. Appl. Microbiol. Biotechnol. 93, 117–129.
Seetharaman, S., McLean, A., Guthrie, R., Sridhar, S., 2014. Treatise on process Metallurgy, Process Phenomena, 2. Elsevier, Oxford, UK p. 199.
Šimčík, M., Mota, A., Ruzicka, M.C., Vicente, A., Teixeira, J., 2011. CFD simulation and experimental measurement of gas holdup and liquid interstitial velocity in internal loop airlift reactor. Chem. Eng. Sci. 66, 3268–3279.
Stafford, D.A., 2001. The effect of mixing and volatile fatty acid concentrations on anaerobic digestion performance. Biomass 2, 43–55.
Stevenson, P., Li, X., 2014. Foam Fractionation, Principles and Process Design. Talyor and Francis group, CRC press p. 113.
Stroot, P.G., Mcmahon, K.D., Mackie, R.I., Raskin, L., 2001. Anerobic codigestion of municipal solid waste and biosoilds under various mixing conditions- I. Digester performance. Water. Res. 35 (7), 1804–1816.
Terashima, M., Goel, R., Komatsu, K., Yasui, H., Takahashi, H., Li, Y.Y., Noike, T., 2009. CFD simulation of mixing in anaerobic digesters. Bioresour. Technol. 100 (7), 2228–2233.
Vesvikar, M.S., Al-Dahhan, M., 2005. Flow pattern visualization in a mimic anaerobic digester using CFD. Biotechnol. Bioeng. 89 (6), 719–732.
Wu, B., 2009. CFD analysis of mechanical mixing in anaerobic digesters. Trans. ASABE 52 (4), 1371–1382.
Wu, B., 2010. CFD simulation of mixing in egg-shaped anaerobic digesters. Water Res. 44 (5), 1507–1519.
Wu, B., Chen, S., 2008. CFD simulation of non-Newtonian fluid flow in anaerobic digester". Biotchnol. Bioegin 99 (3), 700–711.
Yawalkar, A.A., Vishwas, G., Pangarkar, V.G., Anthony Beenackers, A.A.C.M., 2002. Gas Hold-Up in Stirred Tank Reactors. Can. J. Chem. Eng. 80, 158–166.
Ying, K., Zimmerman, W.B., Gilmour, D.J., 2014. Effects of CO and pH on growth of the microalga Dunaliella salina. J. Microb. Biochem. Technol. 6 (3), 167–173.
Ying, K., Gilmour, D.J., Shi, Y., Zimmerman, W.B., 2013a. Growth enhancement of *Dunaliella salina* by microbubble induced airlift loop bioreactor (ALB)—the relation between mass transfer and growth rate. J. Biomater. Nanobiotechnol. 4 (2A), 1–9.
Ying, K., Al-Mashhadani, M.K.H, Hanotu, James O., Gilmour, D.J., Zimmerman, W.B., 2013b. Enhanced mass transfer in microbubble driven airlift bioreactor for microalgal culture. J. Eng. 5 (9), 735–743.
Zayas, J.F., 1997. Functionality of Proteins in Food. Springer-Verlag, Berlin Heidelberg p. 274.
Zimmerman, W.B., Zandi, M., Bandulasena, H.C.H., Tesař, V., Gilmour, D.J., Ying, K., 2011a. Design of an airlift loop bioreactor and pilot scales studies with fluidic oscillator induced microbubbles for growth of a microalgae *Dunaliella salina*. Appl. Energy 88, 3357–3369.
Zimmerman, W.B., Hewakandamby, B.N., Tesar, V., Bandulasena, H.C.H., Omotowa, O.A., 2009. On the design and simulation of an airlift loop bioreactor with microbubble generation by fluidic oscillation. Food Bioprod. Process 87, 215–227.
Zimmerman, W.B., Václav Tesař, H.C., Bandulasena, Hemaka, 2011b. Towards energy efficient nanobubble generation with fluidic oscillation. Curr. Opin. Colloid Interface Sci. 16 (4), 350–356.